Talanta 131 (2015) 74–80

Contents lists available at ScienceDirect

Talanta

journal homepage: www.elsevier.com/locate/talanta

Analyzing the biosensor signal in flows: Studies with glucose optrodes

K. Kivirand [a], A. Floren [b], M. Kagan [a], T. Avarmaa [b], T. Rinken [a], R. Jaaniso [b,*]

[a] Institute of Chemistry, University of Tartu, Ravila 14a, Tartu 50411, Estonia
[b] Institute of Physics, University of Tartu, Ravila 14c, Tartu 50411, Estonia

ARTICLE INFO

Article history:
Received 6 April 2014
Received in revised form
15 July 2014
Accepted 21 July 2014
Available online 30 July 2014

Keywords:
Modeling
Dual-optrode biosensor
Flow regime
Glucose
Pre-steady state calibration

ABSTRACT

Responses of enzymatic bio-optrodes in flow regime were studied and an original model was proposed with the aim of establishing a reliable method for a quick determination of biosensor signal parameters, applicable for biosensor calibration. A dual-optrode glucose biosensor, comprising of a glucose bio-optrode and a reference oxygen optrode, both placed into identical flow channels, was developed and used as a model system. The signal parameters of this biosensor at different substrate concentrations were not dependent on the speed of the probe flow and could be determined from the initial part of the biosensor transient phase signal, providing a valuable tool for rapid analysis. In addition, the model helped to design the biosensor system with reduced impact of enzyme inactivation to the system stability (20% decrease of the enzyme activity lead to only a 1% decrease of the slope of the calibration curve) and hence significantly prolong the effective lifetime of bio-optrodes.

1. Introduction

Biosensors are analytical devices incorporating a bio-recognition element and a physical transducer for the detection of target compounds. The transducer converts the recognition event into a measurable signal and can be of different type: electrochemical, optical, thermal or piezoelectrical. Most enzymatic biosensors are based on electrochemical transducers [1], which, in case of catalytic red-ox reactions, sense directly the charge transfer or detect the consumption of O_2 or generation of H_2O_2 in the reaction. At the same time, there is an increasing interest in optical transducers [2–4], in particular those detecting O_2 and H_2O_2 in solutions. Optical sensors have several advantages: they are resistant to electrical and electrochemical interferences, allow non-contact sensing or transmission of parallel sensor signals over a single optical fiber, and have relatively long service interval [5].

Irrespective of the specific nature of bio-recognition processes and signal transduction mechanisms, biosensors are ideally expected to perform as the regular physical sensors – that is to operate continuously, reversibly and rapidly, giving accurate information in real or near real-time and facilitating on site applications. This implies that all the sensor components (platform, bio-recognition entities, transducer, signal conditioning unit) are carefully engineered and the transfer function of the sensor is described by adequate model.

The basic tool for modeling enzymatic biosensors is the convection–diffusion-reaction equation (or a system of such equations), which is numerically solved for given boundary and initial conditions [6–14]. These conditions depend on several aspects: the geometry of the sensor, location of the enzyme (immobilized or distributed in solution), transducer type, and mode of liquid motion (batch or flow-through regime). Flow-through systems, e.g. those used for flow injection analysis (FIA), are advantageous as allowing high sample throughput and overall reduction of the analysis time [15,16]. Whereas most of the recent modeling efforts are devoted to describing the sensor performance in flow regime, all these efforts are still made (and valid) only for amperometric transducers. Therefore, for optimizing the construction of optical biosensors and for detailed signal analysis of such sensors specially targeted studies have to be undertaken.

In the present work, we are investigating the flow-through enzymatic biosensor with fiber-optic optrodes (or optodes) based on luminescence quenching by oxygen. Such bio-optrodes have been introduced in Ref. [17] and further developed in Refs. [18–25] in parallel with industrial [26], biological [27], and medical [21,28,29] applications. In order to analyze correctly the signal of such biosensor, one has to know the actual level of dissolved oxygen in the probe, and therefore the dual-optrode sensing has been introduced [19–21], which uses an enzyme-activated optrode together with a reference optrode for oxygen.

The main goal of the present work was to develop a simple but sufficiently accurate model for describing the response of optical

* Corresponding author. Tel.: +372 7374731.
E-mail address: raivo.jaaniso@ut.ee (R. Jaaniso).

http://dx.doi.org/10.1016/j.talanta.2014.07.061
0039-9140/

enzymatic biosensor operating in flow regime. To achieve this, we constructed a stable dual-optrode biosensor; carried out experiments with glucose optrodes, using glucose oxidase for glucose detection; developed a model for describing the sensor response, and fitted the experimental data with the theoretical curves. The development of the model was aimed for obtaining the analytical transfer functions for the sensor, which could be used for calibration and signal processing in practical devices.

2. Experimental

2.1. Dual-optrode biosensor system with flow cell

The scheme of the dual-optrode biosensor is shown in Fig. 1. The system consists of two optrodes, flow cell, heater, opto-electronic unit, and control unit. The glucose and reference optrodes were placed into isolated identical flow channels (l=50 mm; Ø=3 mm) of the carefully thermostated flow cell. The opto-electronic unit provided optical excitation (wavelength 405 nm) of luminescence, as well as the detection and amplification of luminescence signals (wavelength 690 nm) from optrodes. The optrodes were connected to the unit through plastic coated quartz fibers (Ø=1 mm, NA=0.37) supplied with SMA connectors.

As the analytical performance of the biosensor was anticipated to be greatly dependent on temperature [21,30], the stabilization of the cell temperature was one of the most crucial issues of the experimental setup: so a high-precision temperature sensor (RTD, class A) was placed into a similar flow channel and connected with the control device of the Kapton® (polyimide film) insulated flexible heater surrounding the flow cell. The control unit was connected to PC via USB interface and included ADCs for signal conversion, *I/O* ports for switching the LEDs for luminescence excitation, and PID regulator for heater.

The bio-optrode and reference optrode were placed into identical flow channels, which allows to make precise differential or ratiometric measurements and hence minimize the influence of experimental noise like occasional oxygen fluctuations in the flow, caused by adverse effects such as bacterial growth; temperature fluctuations; or pressure fluctuations of the peristaltic pump.

The oxidation of glucose, catalyzed by glucose oxidase was studied as a model reaction:

$$\beta - D - \text{glucose} + O_2 \xrightarrow{\text{Glucoseoxidase}} \delta - \text{lactone} + H_2O_2. \quad (1)$$

2.2. Preparation of the bio-optrodes

The oxygen optrodes used were based on optical quartz fibers, which were dip-coated with oxygen-sensitive films. The detection of oxygen was based on measuring the phosphorescence quenching of Pd-tetraphenylporphyrin molecules, encapsulated into a polymethyl methacrylate (PMMA) film [31]; the latter covering the cylindrical surface of a 30 mm long optical fiber with diameter of 1 mm. Pd-porphyrin (Porphyrin Systems) and PMMA polymer (molar mass 40,000 g/mol, Sigma-Aldrich) were dissolved in chloroform or tetrahydrofuran, the solutions were treated on ultrasonic bath and filtered through a teflon filter with 1 μm pore size. After dip-coating, the fiber-tips were dried at room-temperature for some hours and aged at 60 °C for ~1 month [31,32].

Glucose oxidase (GOD, EC 1.1.3.4. from *Aspergillus niger*, 17,300 U/g protein, Sigma-Aldrich) was immobilized onto the threads made of nylon-6,6, according to a previously published protocol [33] with some minor modifications. Nylon threads (consisting of 60 filaments with a diameter of 25 μm twisted together) were immersed into 98% (w/w) dimethyl sulfate for 10 min at 50 °C, washed several times with ice-cold methanol and 0.1 M phosphate buffer (PB) (pH 6.50) and immersed into 12.5% glutaraldehyde solution (in 0.1 M PB, pH 6.50) for 1 h at room temperature. The activated threads were washed with 0.1 M PB (pH 6.50) and incubated in GOD solution (100 U/ml), first for 2 h at room temperature and then overnight at 4 °C. Finally, the threads were thoroughly washed and stored in 0.1 M PB (pH 6.50) at 4 °C.

For the preparation of a glucose optrode, 19 cm of GOD-containing thread with initial catalytic activity 0.016 U/cm was cut and coiled around the oxygen-sensitive surface of the oxygen optrode, where it formed a bio-recognition layer for glucose

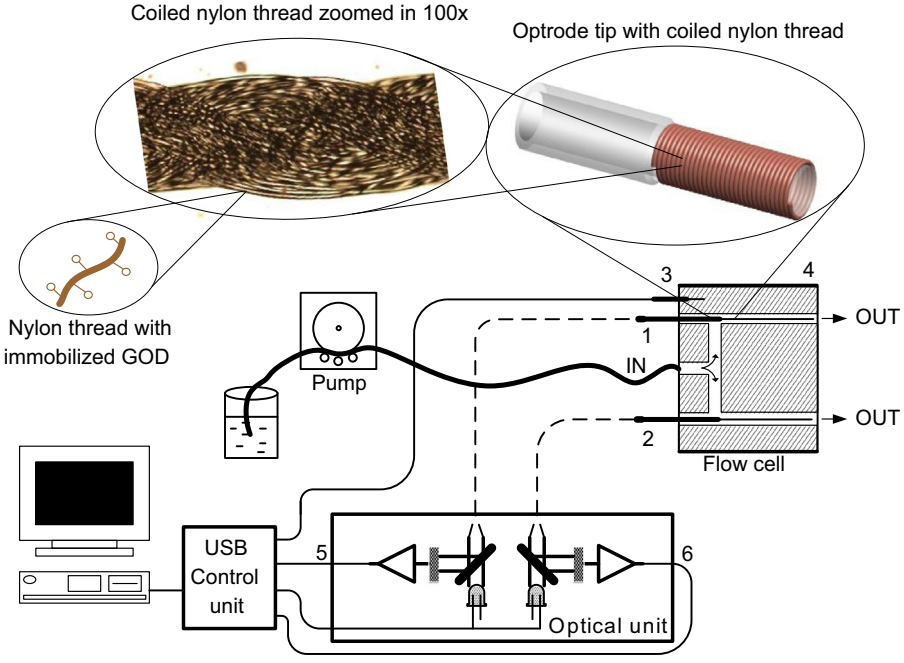

Fig. 1. Scheme of dual-optrode biosensor system: 1—glucose bio-optrode; 2—reference optrode; 3—temperature sensor; 4—Kapton flexible heater; 5 and 6—electronic signals from two detection channels. Optical fibers are shown with dashed lines. Insets show magnified scheme and image of optrode.

[34,35]. The catalytic activity of the thread was tested before each series of measurements. If the activity dropped below 80% of its initial value, the GOD-containing thread was replaced. The reference oxygen optrode was covered with 19 cm of identical "blank" thread.

2.3. Measurement procedures and data acquisition

Glucose stock solutions were prepared in 0.1 M phosphate buffer (PB) (pH 6.50) and allowed to mutarotate overnight along with their aeration with air at 37 °C; glucose solutions were prepared into air-saturated PB (at 37 °C) immediately prior to use. All reagents used were of analytical grade.

To minimize the influence of bubble forming on the biosensor signal, the inflow of the solution was in the bottom and the outflow in the upper part of the cell. The flow rate of the measurements was varied from 0.8 ml/min to 13.0 ml/min. The average flow velocities in the channels of the flow cell were estimated to be between 0.3 to 4.8 cm/sec, taking into account the free cross-section of a channel (4.5 mm^2). After each measurement the system was washed with 0.1 M PB (pH 6.50) until the sensor signals reached their initial values.

The flow cell was thermostated at 37.0 ± 0.1 °C. This temperature was optimal to gain the highest biosensor sensitivity at reasonable dissolved oxygen concentration (DOC) levels in the studied solutions. The dual-sensor response for glucose was found as the ratio of DOC at bio-optrode and reference optrode at every time moment measured, so minimizing the impact of experimental noise.

The sensor signal was recorded with the interval of 1 s between the consecutive data points; each experimental curve consisted of at least 300 data points. The dissolved oxygen concentration was calculated on the basis of Stern–Volmer relationship *[36]*, using original software Oxysens 2.0. The software also controlled the system and allowed automated measurements. In particular, it allowed to set and record the measurement temperature, and took into account the temperature corrections, required for accurate determination of DOC. The temperature dependence of Stern–Volmer coefficient, determined earlier in Ref. *[31]*, was used.

3. Model

In the flow cell, there are generally two processes governing the oxygen concentration at the optrode surface:

1) enzyme-catalyzed reaction in the enzyme containing layer;
2) transport of oxygen and the second substrate into and in the flow cell.

The studied reaction (1) is of ping-pong type [37] and can be described in the quasi-steady-state approximation as following:

$$\frac{ds(t)}{dt} = \frac{dc(t)}{dt} = -\frac{V_{MAX}}{1+\frac{K_S}{s(t)}+\frac{K_{O_2}}{c(t)}}, \tag{2}$$

where $s(t)$ is the substrate concentration, and $c(t)$ is DOC at time moment t; K_S and K_{O_2} are Michaelis' constants for substrate and oxygen, respectively; and V_{MAX} is the ultimate reaction speed.

If the following condition is fulfilled:

$$\frac{K_S}{s} \gg 1+\frac{K_{O_2}}{c}, \tag{3}$$

Eq. (2) can be simplified to:

$$\frac{ds(t)}{dt} = \frac{dc(t)}{dt} = -k_R s(t), \tag{4}$$

where

$$k_R = \frac{V_{MAX}}{K_S}. \tag{5}$$

For glucose oxidation $K_S \gg K_{O_2}$ [37], and therefore condition (3) is fulfilled in a quite wide range of β-D-glucose and oxygen concentrations. The upper limit of oxygen concentration is generally determined by its saturated value ($c_0 \sim 0.2$–0.3 mM at temperatures 20–40 °C). In what follows, we will assume the reaction to be described by first order kinetics (4), and as we will see below, this approach is justified even at substrate concentrations exceeding several times the value of c_0.

Regarding the transport processes, the addition of substrate and oxygen into the vicinity of sensor surface will be described in the model with linear kinetic terms. Then the overall process can be modeled by two kinetic equations:

$$\frac{ds(t)}{dt} = -k_R s(t) + k_S[s_0 F(t) - s(t)] \tag{6}$$

$$\frac{dc(t)}{dt} = -k_R s(t) + k_{O_2}[c_0 - c(t)] \tag{7}$$

The rate constants k_S and k_{O_2} characterize the exchange speed of the concentrations of substrate and oxygen, respectively, between the flowing liquid and sensor surface (see Fig. 2). We note that similar phenomenological description of transport has been previously successfully used, for example, in modeling of BIACORE experiments [38].

It is assumed here, that oxygen concentration in the flowing liquid entering the cell is always c_0, and after passing the initial front, the substrate carried by liquid flow has constant concentration s_0. The function $F(t)$ describes the arrival front of the substrate into the cell. When the passage of the front is fast compared to the reaction and transport processes, then $F(t)$ can be approximated by Heaviside function:

$$F(t) = H(t) = \begin{cases} 0, t < 0 \\ 1, t \geq 0 \end{cases}. \tag{8}$$

We also assume that there is no substrate present in the cell before $t=0$. Under these conditions the solutions of Eqs. (6) and (7) are:

$$s(t) = s_0 k_S \int_0^t dt' \exp\left[(k_R + k_S)(t' - t)\right], \tag{9}$$

$$c(t) = c_0 - k_R \int_0^t dt' s(t') \exp[k_{O_2}(t' - t)]. \tag{10}$$

After inserting Eq. (9) into (10) and evaluating the integrals one obtains:

$$c(t) = c_0 - s_0 \frac{k_R k_S}{k_{SR} k_{O_2}} \left\{ 1 - \exp(-k_{O_2} t) + \frac{k_{O_2}}{k_{O_2} - k_{SR}} \left[1 - \exp(-k_{SR} t) \right] \right\}, \tag{11}$$

where we used the notation

$$k_{SR} = k_S + k_R. \tag{12}$$

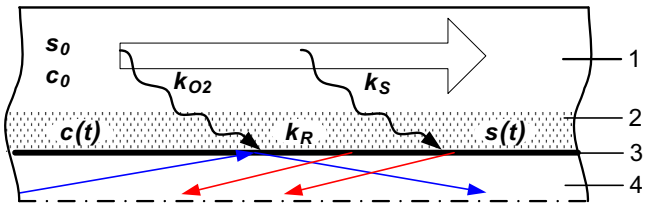

Fig. 2. Cross-section of the flow cell and scheme of model processes. 1- flowing liquid; 2 – flossy coating containing immobilized enzyme molecules; 3 – oxygen sensitive coating; 4 – core of optical fiber. The arrows inside the fiber represent the light involved in optical oxygen sensing.

The stationary solution for DOC is:

$$c_f = \lim_{t\to\infty} c(t) = c_0 - s_0 \frac{k_R k_S}{k_{SR} k_{O_2}} \tag{13}$$

The Eq. (11) can be rewritten in a following form:

$$\frac{c(t)}{c_0} = 1 - A \cdot f(t), \tag{14}$$

where

$$f(t) = 1 - \frac{k_{SR}}{k_{SR} - k_{O_2}} \exp(-k_{O_2} t) + \frac{k_{O2}}{k_{SR} - k_{O_2}} \exp(-k_{SR} t) \tag{15}$$

is the normalized function describing the temporal evolution of relative DOC. It is easy to verify that it is a monotonic function changing from zero to unity i.e. $f(0) = 0$ and $\lim_{t\to\infty} f(t) = 1$.

Parameter A gives the relative difference between the initial (c_0) and final stationary (c_f) oxygen concentrations and can be easily determined experimentally as a normalized change of DOC between the initial and final steady states:

$$A = \frac{c_0 - c_f}{c_0} = \frac{s_0 k_R k_S}{c_0 (k_S + k_R) k_{O_2}}. \tag{16}$$

4. Comparison of sensor response with the model

A series of sensor responses, recorded at different glucose concentrations in two flow channels are shown in Fig. 3. At constant saturated DOC, the response of the reference sensor was not dependent on glucose concentration, while the response of the glucose biosensor decreased due to consumption of oxygen according to reaction (1). One can see five pairs of response and recovery curves taken successively at a flow rate of 2.7 ml/min. The arrows mark the time moments, when the substrate was added. The duration of substrate injection was 300 s and thereafter the signal was restored in the flow of pure buffer solution to the initial level.

In Fig. 4, a closer look at the (normalized) response curves at four different glucose concentrations is given together with the model curves obtained by fitting with Eqs. (14), (15). For each curve, the parameter A and two rate constants, k_{O_2} and k_{SR}, were determined. The application of the model for the characterization of the biosensor output signal resulted in good correlation ($R^2 = 99\%$, standard deviations from the model 0.00077, p-value < 0.0001). As one can see in Fig. 4, at the beginning of the response curves the signal decreases relatively slowly, whereas

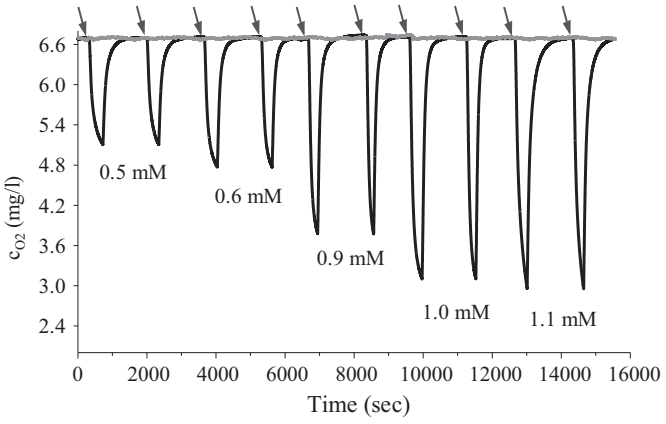

Fig. 3. Response curves of glucose bio-optrode (black line) and the reference optrode (gray line) of consecutive measurements at different glucose concentrations (two measurements at each concentration). Measurements were carried out at 37 °C in 0.1 M phosphate buffer (pH 6.50) at flow rate 2.7 ml/min. Arrows indicate the time of adding the substrate solution.

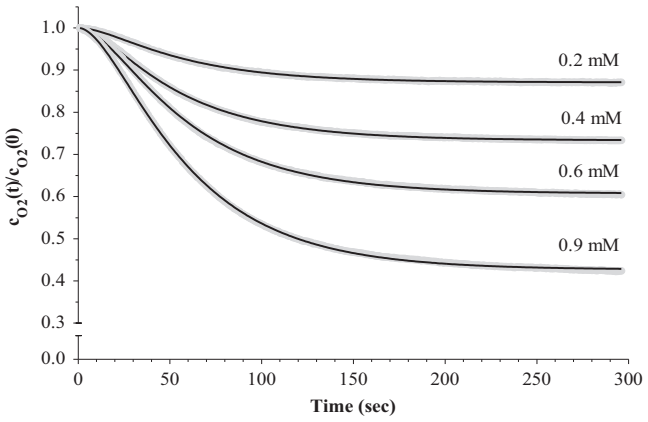

Fig. 4. Fitting the experimental curves (gray) obtained at different glucose concentrations (0.2 mM; 0.4 mM; 0.6 mM; 0.9 mM) with the proposed model. Theoretical approximations are shown as solid black lines. Measurements were carried out at 37 °C in 0.1 M phosphate buffer (pH 6.50) at flow rate 2.7 ml/min.

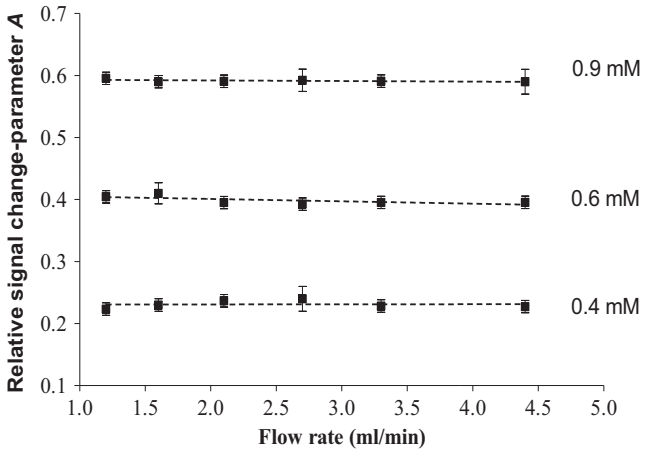

Fig. 5. The relative signal change parameter at different glucose concentrations and flow rates. Measurements were carried out at 37 °C in different glucose solutions in 0.1 M phosphate buffer (pH 6.50).

this change is accelerating. Such behavior is caused by the lack of substrate in the enzyme-containing layer at the initial moment and is accurately described by the model.

Parameter A characterizes the biosensor steady-state response (see Eq. (16)), which is the most common information used in biosensor studies [39]. It can be simply estimated by recording the initial and final steady state signals. Such procedure – determining the change of steady state signal (or the presumed 95% of it) versus substrate concentration - is the most common way of calibrating and using the biosensors. However, the fitting of temporal response curves, as demonstrated in Fig. 4, provides not only more accurate way of determining parameter A, but also valuable information included in rate constants.

For characterizing the processes in the flow system, the dependence of parameter A on flow rate at different glucose concentrations was studied (Fig. 5). As one can see, the value of parameter A was practically independent on the flow rate in the studied range of 0.8 to 13.0 ml/min. This result has an important practical consequence: it allows constructing universal calibration curves, not dependent on the flow rate in the system. We will discuss the interpretation of this result later; at this point we note in addition, that it was not possible to carry out experimental measurements at small flow rates (under 0.8 ml/min) due to the accumulation of air bubbles in the cell. In what follows, the results

obtained at a medium flow rate of 2.7 ml/min are mainly used as examples.

The determined values of parameter A were used for biosensor calibration. The slope of the calibration curve was calculated separately for every studied flow rate and no statistically significant differences in the slope values at different flow rates were detected. The glucose calibration curve at flow rate 2.7 ml/min possessing a linear dependence with the slope (0.701 ± 0.008) mM^{-1} ($R^2 = 0.997$) is shown as an example in Fig. 6. The absence of constant term in this dependence indicates the lack of systematic errors in the results.

Let us now remind that in addition to parameter A, two rate constants were determined from each response curve. For example, fitting the experimental curves shown in Fig. 3 with Eq. (15) resulted the values 0.023 s^{-1} and 0.068 s^{-1} for two rate constants. One of these values characterizes the oxygen transport (k_{O_2}) and the second one the combined effect of reaction and substrate transport (k_{SR}). However, because the Eq. (15) is symmetric with respect of two rate constants (formula remains the same at the interchange $k_{O_2} \leftrightarrow k_{SR}$), one requires additional information for assigning the determined rate values to one or another particular process.

Furthermore, the procedure of evaluating the rate parameters of individual processes, k_S andk_R, should be established. Inserting k_R from Eq. (12) into Eq. (16) one gets a quadratic equation for k_S. The solution of this equation is:

$$k_S = \frac{k_{SR}}{2} \pm \sqrt{\left(\frac{k_{SR}}{2}\right)^2 - A\frac{c_0}{s_0}k_{SR}k_{O_2}}, \qquad (17)$$

which allows to calculate the substrate transport rate k_S from the values of parameters (A, k_{O_2} and k_{SR}) obtained from fitting the experimental data. For this calculation only such assignment of k_{O_2} and k_{SR} values is reasonable, which results positive (or zero) value of the expression under the square root in Eq. (17). In case of our experimental data this condition was found to be satisfied only when $k_{SR} > k_{O_2}$. This condition solves the problem due to Eq. (15) symmetry and allows fixing the value of k_{O_2}. Still, as Eq. (17) gives two solutions (with plus and minus signs, respectively), one should define an additional criterion for the determination of unique set of rate parameters k_S and k_R.

At this point, it should be reminded that the values of A (as well as the values of k_{O_2} and k_{SR}) were independent on the flow rate. This fact indicates that in the studied flow rate range the mass transfer was entirely limited by the transport (diffusion) in the layer of enzyme carrier. As the diffusion rates are inversely proportional to the molecular dimensions (Stokes radii), the following condition should hold for oxygen and glucose: $k_{O_2} > k_S$. This condition is satisfied only for the solution of Eq. (17) with minus sign and hence assures unique determination of parameters.

Following the rules, established above for the relative magnitude of the rate parameters, we calculated the transport rates for oxygen and glucose, k_{O_2} and k_S respectively, for every biosensor response curve. These coefficients were not dependent on the glucose concentration or the flow rate of the analytes and their mean values, calculated from different measurements were not significantly different. The mean values of k_{O_2} and $k_S$were found to be 0.022 (SD=0.003) s^{-1} and 0.0030 (SD=0.0004) s^{-1}, respectively. Finally, the reaction rate was obtained from Eq. (11), which resulted $k_R = 0.065$ (SD=0.004) s^{-1}. The value of the ratio k_{O_2}/k_S, supposedly indicating the relationship of molecular radii of glucose and oxygen molecules, was between 5.9 and 7.9. This result is in a good correlation with the ratio of van der Waals' radius of oxygen (1.52 Å) and molecular size of glucose (10 Å), equaling to 6.6.

To conclude, we demonstrated that the model describes the sensor responses adequately and allows: (1) clear interpretation of underlying processes; (2) easy biosensor calibration from pre-steady-state data. In this final paragraph of the section we explore the last feature further: we demonstrate how and in which limits the pre-steady-state data can be used for shortening the measurement time. For this purpose we fitted the temporal responses (shown in Fig. 4) within different time intervals (the curves were fitted between $t=0$ and $t=t_F$, whereas t_F was varied from 300 s to a minimal value of ~20 s). This allowed simulating the situation, where the sensor output value is determined from shorter and shorter measurements. The results for parameter A, determined at three different substrate concentrations, are presented in Fig. 7. It is evident, that in all cases the parameter A is practically constant down to the measurement time t_F ~60 s. In Fig. 7, the data for two fitting procedures are presented. The filled dots present the data obtained when all parameters (A, k_{SR}, and k_{O_2}) in Eqs. (14,15) were freely varied, whereas the empty dots present the data obtained when the rate parameters were fixed (as determined at previous calibration) and only parameter A was varied. As one can see, by using the fixed set of pre-calibrated rate parameters, the measurement time can even be as short as 20 s. In other words, for

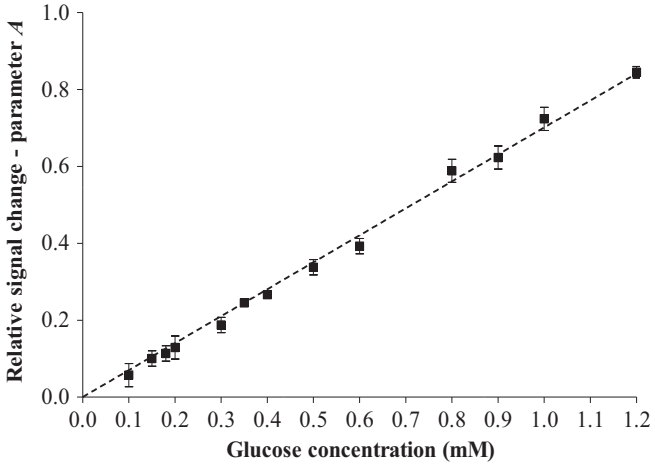

Fig. 6. The dependence of the relative signal change parameter A on glucose concentration. Measurements were carried out at 37 °C in 0.1 M phosphate buffer (pH 6.50) at flow rate 2.7 ml/min.

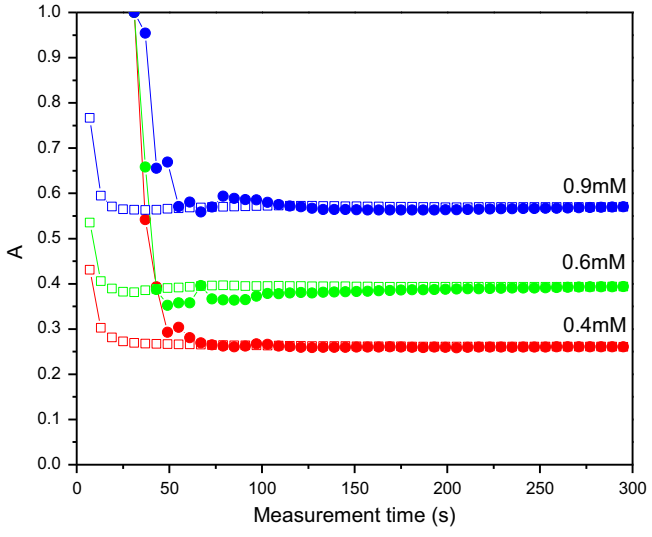

Fig. 7. The dependence of parameter A on the measurement time. Measurements were carried out at 37 °C in 0.4 mM, 0.6 mM, and 0.9 mM glucose solutions in 0.1 M phosphate buffer (pH 6.50) at flow rate 2.7 ml/min. At fitting, all three parameters (filled dots) or only parameter A (open dots) was freely varied.

obtaining the parameter A (and then the substrate concentration from the calibration curve presented in Fig. 6) there is no need to record the signal up to 300 s but the recording time can be as short as 20 s. Note that these concrete values of characteristic times are related to concrete bio-optrodes and may hence vary between different systems, e.g. the optrodes with higher enzyme activity will have higher reaction rate, which leads to shorter characteristic times as well. If we look at the fitting results in Fig. 7 and at the signal changes in Fig. 4 in parallel, more general criterion may be formulated. In Fig. 4 one observes that the relative signal dropped at 20 and 60 s by ~20% and ~50%, respectively. In conclusion, one can determine the substrate concentrations by measuring the signal until it has dropped only by 20–50% of its maximal (steady-state) change, and not waiting until the signal change has reached the 95% level of the presumed final change. This presents a significant advantage, as the measurement time can be shortened more than by one order in magnitude.

5. Discussion

Modeling of biosensor signals in flows is usually based on the diffusion-advection-reaction equation, which can be generally solved only by numerical methods [7–14]. Analytical solutions have been found only in few special cases [40]. In case of two-substrate reactions (1), one has even more complicated situation, described by a system of two coupled diffusion-advection-reaction equations.

As it is described in previous sections, a more simple approach based on ordinary rate equations allowed to evaluate the biosensor signals well not only qualitatively (providing clear interpretation of the response curves as well as such basic characteristics as sensitivity and stability, see below) but also quantitatively (providing enough precision even for pre-steady-state data). For understanding the success of this approach, an analogy with thermal transport problems can be drawn. Thermal problems are generally governed by an analog of diffusion equation but frequently a more simple approach with ordinary differential equation is used with rate parameters determined by thermal conductance and capacity. The advantage of rate equations is similar in both problems: simple analytical solutions provide clear and transparent interpretation and easy calculation procedure. Of course, the simplified description of the problem can be used only within certain parameter limits, which guarantee required precision for a given practical application. In the present case, for example, the model is valid until the processes of advection and diffusion in the solution outside the layer of enzyme carrier start to play a bigger role. This means that the model cannot be applied at very low flow rates or for describing the measurements in the stopped-flow regime. However, in the flow regime the model was completely adequate in a wide range of the flow rates.

The independence of model parameter A (describing the relative signal change) from the flow rate indicated that the transport is limited by diffusion in the layer of enzyme carrier and the advection in the flow channel is relatively fast. Previously we gave a coarse estimate of the ratio of diffusion rates based on molecular sizes. More precisely, the diffusion rates are given by the inverse values of characteristic diffusion times through a layer with thickness d:

$$k_{O_2} = D_{O_2}/d^2$$
$$k_S = D_S/d^2 \quad (18)$$

Here D_{O_2} and D_S are the diffusion coefficients of oxygen and substrate, respectively, in the enzyme carrier. Therefore we have

$$k_{O_2}/k_S = D_{O_2}/D_S \quad (19)$$

From the literature one can find that in the water at 37 °C $D_{O_2} = 2.7 \times 10^{-5}$ cm^2/s [41] and $D_S = 0.9 \times 10^{-5}$ cm^2/s [42]. These values lead to the ratio of diffusion coefficients equal to 3, whereas higher value has been found from our experiments – about 7. This discrepancy can be explained by somewhat preferential deceleration of glucose diffusion inside the flossy nylon thread. For example, in hydrogels [43] both the oxygen and glucose diffusion become slower as compared to water environment, whereas the effect is about twice stronger for glucose. This results in a similar ratio of diffusion rates as found in our study. Taking into account the thickness of the thread $d = 0.3$ mm, one can estimate the diffusion coefficients in the buffer-filled nylon threads at 37 °C: after inserting the experimental transfer rates ($k_{O_2} = 0.022$ s^{-1} and $k_S = 0.003$ s^{-1}) into Eq. (18) one obtains $D_{O_2} = 2.0 \times 10^{-5}$ cm^2/s and $D_S = 0.27 \times 10^{-5}$ cm^2/s.

The most crucial parameter of a sensor is its sensitivity. In the present case the maximal (initial) sensitivity follows from Eq. (16), and is given by

$$S = \left|\frac{dc_f}{ds_0}\right| = \frac{k_R}{k_S + k_R}\frac{k_S}{k_{O_2}} \quad (20)$$

This can be compared with the sensitivity of a system, where the reaction takes place in a closed volume with distributed enzyme and fast mixing of components. Then a simple equation $c_f = c_0 - s_0$ holds for the reaction (1), and the sensitivity $S = 1$. It follows from Eq. (20), that the sensitivity is generally lower for a flow system. The maximal sensitivity of the latter can be achieved if $k_R \gg k_S$ and is then determined by the ratio k_S/k_{O_2}. The latter ratio is given by Eq. (19) i.e. it is determined by the ratio of diffusion coefficients, and therefore can hardly be increased by the design of the sensor. The only way to maximize the sensitivity is to fulfill the condition $k_R \gg k_S$ i.e. by increasing the reaction rate (enzyme activity) above a certain limit. Note that in our system the activity of the immobilized enzyme was high enough to gain sufficiently high bio-optrode activity and reaction rate (k_R was 20 times bigger than k_S). This can be estimated as an optimal situation, as at too high reaction rates the condition set by Eq. (8) becomes invalid, in other words – a more realistic description of arrival front has then to be included into the model. In our studies the passage time of the solution's initial front was 1–3 s, which was short enough to be neglected as compared to the characteristic reaction time $1/k_R = 15$ s.

The condition $k_R \gg k_S$ also assures high stability of the sensor. For example, if the enzyme activity and accordingly the reaction rate decreases by 20% (from 0.065 s^{-1} to 0.052 s^{-1}), the sensitivity (Eq. (20)) and equally the slope of the calibration curve in Fig. 6 change just by 1%. Furthermore, the system sensitivity does not drop below 90% of the initial one even in the case only 30% of the initial enzymatic activity is remaining. Consequently, the actual design of the flow-through biosensor enables to prolong the effective lifetime of optrodes, commonly quite limited due to the inactivation of the bio-selective material and the consequent loss of system sensitivity. Finally, it is worth to remind that the signal stability of the current biosensor design is also warranted (further improved) by the lack of flow-rate dependence and elimination of drifts common to sensing and reference channels.

The model can be applied to other set-ups as well as far as two general conditions are fulfilled: (i) exponential reaction law, resulting from Eq. (3); (ii) diffusion-limited transport of substrates. If these conditions are met, the model can be directly applied for other 2-substrate enzymes, immobilized on other carriers with different procedures as well. The concrete parameters, k_R, k_S, and k_{O_2}, will have different values of course, for each particular set-up, and have to be determined by due calibration. Moreover, these parameters are generally temperature dependent and when the sensor is to be used at different temperatures, the calibration should be performed in the full actual temperature range.

The validity of condition (i) depends on the values of Michaelis' constants K_S and K_{O_2}, and can be estimated for each particular enzyme, whereas the immobilization may change the situation in some degree [1]. The condition (ii) requires the presence of a substrate-permeable layer (thread, gel [18], sol–gel [20], or polymer [21] coating) between the probe liquid and enzymes. Note that with this layer one can engineer the sensitivity, stability and dynamic range of the biosensor.

6. Conclusions

Dual-channel biosensor with fiber-optical oxygen transducers was constructed and used as a model system for studying the biosensor transfer (sensing) functions in flows on the example of glucose oxidase catalyzed reaction. The transducers and the flow cell of the sensor system were designed to match the thread-type enzyme carriers. A mathematical model involving two-substrate reaction (e.g. oxidase-catalyzed reactions, glucose oxidation in particular) and mass transport of substrates was developed for describing the sensor signal. The model is based on a system of rate equations and has a relatively simple analytical solution. This facilitated the interpretation of the experimental sensor data and allowed to develop a method for determining the biosensor output from early pre-steady state signals. It was demonstrated that the sensor reading could be obtained when the signal was changed only by 20% towards its final steady state value, which reduces the detection time about 10-fold as compared to standard procedures (requiring at least 95% signal change). It was established that the sensor parameters did not depend on the flow rate in a relatively wide range (0.8–13 ml/min or 0.3–4.8 cm/s), which showed that the mass transport was determined by diffusion in a flossy layer of substrate carrier. The application of the model to the experimental data also enabled to optimize the biosensor system. It allowed predicting optimal biosensor parameters for obtaining maximal sensitivity and high stability, on one hand, and for achieving fast determination of substrate concentration from pre-steady state data, on the other hand.

Acknowledgments

This work was supported by Estonian Science Foundation Grant no. 9061, Estonian Research Council Grant IUT 20-17, and by the European Regional Development Fund Project “Mesosystems: theory and applications”, 3.2.0101.11-0029.

References

[1] N.J. Ronkainen, H.B. Halsall, W.R. Heineman, Chem. Soc. Rev. 39 (2010) 1747–1763.
[2] J.C. Pickup, F. Hussain, N.D. Evans, O.J. Rolinski, D.J.S. Birch, Biosens. Bioelectron. 20 (2005) 2555–2565.
[3] S. Borisov, O.S. Wolfbeis, Chem. Rev. 108 (2008) 423–461.
[4] M.-S. Steiner, A. Duerkop, O.S. Wolfbeis, Chem. Soc. Rev. 40 (2011) 4805–4839.
[5] M.W. Johnston, J.S. Williams, U.S. Geological Survey Open-File Report 2006-1047, 11 p, 2006, ⟨http://pubs.usgs.gov/of/2006/1047/pdf/ofr2006-1047.pdf⟩.
[6] C.D. Mell, J.T. Maloy, Anal. Chem. 47 (1975) 299–307.
[7] J.K. Leypoldt, D.A. Gough, Anal. Chem. 56 (1984) 2896–2904.
[8] S. Bacha, A. Bergei, M. Comtat, Anal. Chem. 67 (1995) 1669–1678.
[9] J.J. Gooding, Electrochem. Commun. 1 (1999) 119–123.
[10] R. Baronas, F. Ivanauskas, J. Kulys, J. Math. Chem. 32 (2002) 225–237.
[11] J. Lammertyn, P. Verboven, E.A. Veraverbeke, S. Vermeir, J. Irudayaraj, B.M. Nicolai, Sens. Actuators B 114 (2006) 728–736.
[12] V. Flexer, K.F.E. Pratt, F. Garay, P.N. Bartlett, E.J. Calvo, J. Electroanal. Chem. 616 (2008) 87–98.
[13] D. Baronas, F. Ivanauskas, R. Baronas, J. Math. Chem. 49 (2011) 1521–1534.
[14] M.R. Romero, A.M. Baruzzi, F. Garay, Sens. Actuators B 162 (2012) 284–291.
[15] M.I. Prodromidis, M.I. Karayannis, J. Flow Inject. Anal. 21 (2004) 5–10.
[16] M. Bäcker, D. Rakowski, A. Poghossian, M. Biselli, P. Wagner, M.J. Schöning, J. Biotech. 163 (2013) 371–376.
[17] W. Trettnak, M.J.P Leiner, O.S. Wolfbeis, Analyst 113 (1988) 1519–1523.
[18] M.C. Moreno-Bondi, O.S. Wolfbeis, M.J.P. Leiner, B.P.H. Schaffar, Anal. Chem. 62 (1990) 2377–2380.
[19] L. Li, D.R. Walt, Anal. Chem. 67 (1995) 3746–3752.
[20] O.S. Wolfbeis, I. Oehme, N. Papkovskaya, I. Klimant, Biosens. Bioelectron. 15 (2000) 69–76.
[21] A. Pasic, H. Koehler, I. Klimant, L. Schaupp, Sens. Actuators B 122 (2007) 60–68.
[22] V.I. Ogurtsov, J. Hynes, Y. Will, D.B. Papkovsky, Sens. Actuators B 129 (2008) 581–590.
[23] G. Ozturk, S. Timur, S. Alp, Anal. Lett. 41 (2008) 608–618.
[24] S. Nagl, M.I.J. Stich, M. Schäferling, O.S. Wolfbeis, Anal. Bioanal. Chem. 393 (2009) 1199–1207.
[25] C. Zhou, Y. Shi, X. Ding, M. Li, J. Luo, Z. Lu, D. Xiao, Anal. Chem. 85 (2013) 1171–1176.
[26] P.J. Scully, L. Betancor, J. Bolyo, S. Dzyadevych, J.M. Guisan, R. Fernandez-Lafuente, N. Jaffrezic-Renault, G. Kuncova, V. Matejec, B. O'Kennedy, O. Podrazky, K. Rose, L. Sasek, J.S. Young, Meas. Sci. Technol. 18 (2007) 3177–3186.
[27] D.M. Cochran, D. Fukumura, M. Ancukiewicz, P. Carmeliet, R.K. Jain, Ann. Biomed. Eng. 34 (2006) 1247–1258.
[28] Z. Zhou, L. Qiao, P. Zhang, D. Xiao, M.M.F. Choi, Anal. Bioanal. Chem. 383 (2005) 673–679.
[29] A. Pasic, H. Koehler, L. Schaupp, T.R. Pieber, I. Klimant, Anal. Bioanal. Chem. 386 (2006) 1293–1302.
[30] D. Peedel, T. Rinken, Proc. Estonian Acad. Sci. 61 (2012) 306–313.
[31] K. Õige, T. Avarmaa, A. Suisalu, R. Jaaniso, Sens. Actuators B 106 (2005) 424–430.
[32] R. Jaaniso, T. Avarmaa, A. Suisalu, A. Floren, A. Ruudi, K. Õige, Proc. SPIE 5946 (2005) 150–159.
[33] K. Kivirand, T. Rinken, Sens. Lett. 7 (2009) 580–585.
[34] T. Rinken, J. Järv, A. Rinken, Anal. Chem. 79 (2007) 6042–6044.
[35] K. Kivirand, R. Rebane, T. Rinken, Sens. Lett. 9 (2011) 1794–1800.
[36] M. Quaranta, S.M. Borisov, I. Klimant, Bioanal. Rev 4 (2012) 115–157.
[37] Q.H. Gibson, B.E.P. Swoboda, V. Massey, J. Biol. Chem. 239 (1964) 3927–3934.
[38] D.G. Myszka, X. He, M. Dembo, T.A. Morton, B. Goldstein, Biophys. J. 75 (1998) 583–594.
[39] D.A. Baker, D.A. Gough, Anal. Chem. 68 (1996) 1292–1297.
[40] J. Crank, The Mathematics of Diffusion, 2nd ed., Clarendon Press, Oxford, 1975.
[41] A.C.F. Ribeiro, O. Ortona, S.M.N Simoes, C.I.A.V. Santos, P.M.R.A. Prazeres, A.J. M. Valente, V.M.M. Lobo, H.D. Burrows, J. Chem. Eng. Data 51 (2006) 1836–1840.
[42] P. Han, D.M. Bartels, J. Phys. Chem. 100 (1996) 5597–5602.
[43] S.A.M. Van Stroe-Biezen, F.M. Everaerts, L.J.J. Janssen, R.A. Tacken, Anal. Chim. Acta 273 (1993) 553–560.